Pergamon

SCIENCE DIRECT®

Bioorganic & Medicinal Chemistry 11 (2003) 53–58

BIOORGANIC & MEDICINAL CHEMISTRY

GFP-Linked Zinc Finger Protein Sp1: Fluorescence Study and Implication for N-Terminal Zinc Finger 1 as Hinge Finger

Keizo Matsushita and Yukio Sugiura*

Institute for Chemical Research, Kyoto University, Uji, Kyoto 611-0011, Japan

Received 7 May 2002; accepted 20 July 2002

Abstract—The N-terminal zinc finger (zf) of Sp1 is referred to as the 'hinge finger', which connects the C-terminal DNA binding domain with the N-terminal activation domain. In this study, we investigated how a green fluorescent protein (GFP) linked to the N-terminal zinc finger is located spatially. The fluorescence resonance energy transfer technique and steady-state fluorescence anisotropy measurements indicate the results as follows: (1) In the binding to GC-box DNA, the geometry of the GFP domain of the GFP-linked Sp1 zinc finger is similar to that of the Ala-556→Arg mutant. (2) The GFP-linked Sp1 zinc finger is folded more compactly in the absence of DNA (hydrodynamic volume $V = 78.2$ nm^3) and consequently alters the conformation at the GFP domain more extensively ($\Delta V = 43.6$ nm^3) upon DNA binding than the Ala-556→Arg mutant (99.5, 14.8 nm^3, respectively). These results implicate that the N-terminal 'hinge finger' moderates various interactions of the adjacent N-terminal regulation domain with other transcriptional factors as well as DNA binding and is essential for the function of Sp1 and/or Sp/XKLF family members.

Introduction

Human transcription factor Sp1[1] is a C_2H_2-class zinc finger (zf) protein of the Sp/XKLF family containing numerous Krüppel-like factors which conserve three zinc fingers in the C-terminus. Specifically, Sp1 binds to 5′-(G/T)GGGCGG(G/A)(G/A)(C/T)-3′ elements (GC-boxes) within the 5′-flanking promoter sequences and enhances transcription from numerous viral and cellular genes.[2–4] The model for Sp1–DNA interaction had been analogously proposed from the Zif268–DNA interaction mode, determined by the X-ray structure.[4–6] However, some previous studies showed that the DNA binding mode of the N-terminal zinc finger 1 differs between Sp1 and Zif268.[5–9] In Sp1, the finger 1 covers 5 base pairs (bp) DNA and the DNA binding affinity and sequence specificity decrease in the order of finger 3 > finger 2 > finger 1. In Zif268, each finger covers 3–4 bp DNA and the order of contribution for DNA binding is as follows: finger 2 > finger 1 > finger 3.[10] The Ala-556→Arg substitution (Sp1A556R) drastically altered the DNA binding mode and binding specificity of each zinc finger. The mutated finger 1 covers 3–4 bp and the DNA binding specificity decreases in the order of finger 2 > finger 1 > finger 3. That is, the substitution caused the conversion of the Sp1 zinc finger to the Zif268-like finger.[11] Probably, Ala-556 is indispensable in the role as a 'hinge finger' of the N-terminal finger of Sp1.[11]

In order to investigate protein–DNA complexes, fluorescence resonance energy transfer (FRET) has been applied as a powerful tool.[12–14] This principle is based on the fact that energy transfer occurs between two fluorophores when they are in close proximity (10–100 Å), and the emission spectrum of the first fluorophore (the donor) overlaps the excitation spectrum of the second (the acceptor).[15,16] The energy transfer is dependent on the quantum yield of the donor, the degree of spectral overlap, and the orientation of the fluorophores, and declines with the sixth power of the distance. Anisotropy measurements provide important information about rotational motion.[17] The study of the Brownian motion of protein molecules containing their rotational movements indicates their size and shape, and hence this method is suitable for measuring the interaction between proteins and other macromolecules or conformational changes.[17–21]

*Corresponding author. Tel.: +81-774-38-3210; fax: +81-774-32-3038; e-mail: sugiura@scl.kyoto-u.ac.jp

0968-0896/03/$ - see front matter © 2002 Elsevier Science Ltd. All rights reserved.
PII: S0968-0896(02)00337-1

The 27 kD green fluorescent protein (GFP) was identified as the energy acceptor and ultimate emitter in *Aequorea* bioluminescence.[22–24] Because exogenous substrates and cofactors are not required for this luminescence, GFP can be used to monitor gene expression and protein targeting in intact cells and organisms.[24–26] The engineering of GFP variants into chimeric proteins is useful for biosensors, or physiological indicators, and indeed has been applied for FRET and so on.[27–29]

In this report, GFP was employed to mimic the inherent N-terminal transcriptional activation domain neighboring the Sp1 zinc-finger domain. We determined the distances between GFP and fluorescence-labeled DNA by the FRET technique and also the conformation of DNA-free or-bound protein by fluorescence anisotropy. This study indicates that the N-terminal zinc fingers of Sp1 and Sp/XKLF family members affect the orientation and dynamics of the adjacent N-terminal domain as a 'hinge finger'.

Results and Discussion

DNA binding modes of glutathione *S*-transferase (GST) GFPSp1zfs

To evaluate the DNA binding activity and base recognition mode of GSTGFPSp1 wild type (WT) and GSTGFPSp1A556R, gel mobility shift assays and methylation interference analyses with single GC-box DNA were performed. Gel mobility shift assays showed the specific binding of the GSTGFPSp1zfs to the cognate GC-box sequence, but their apparent DNA binding affinities ($K_d = 500$–1000 nM, respectively) were lower than those ($K_d = 10$–30 nM) of the peptide containing only the zinc finger domain of Sp1.[7,11] This result suggests the hindrance of the GSTGFP domain to access the target DNA (e.g., steric hindrance and electrostatic repulsion). The full-length native Sp1 can bind to the GC-box DNA with almost the same affinity as the peptide containing only the zinc finger domain.[5] Probably, the inherent N-terminal activation domain of Sp1 is favorable for or cooperatively supports the binding to the target DNA. On the other hand, methylation interference analyses of GSTGFPSp1WT and GSTGFPSp1A556R gave DNA base recognition modes similar to those of Sp1WT and Sp1A556R, respectively (Fig. S1, Supporting Information, and ref. 11), suggesting no significant effect of the N-terminal GSTGFP moiety on the DNA base recognition mode of Sp1. In the protein-bound sample, non-specific DNA cleavage ladders were detected at non-guanine bases out of the binding site. Intrinsic nuclease activity analyses showed that this cleavage activity for an hour incubation is too weak ($<1\%$). To obtain the conformational information on the GSTGFPSp1zfs, therefore, we adopted the two fluorescence techniques.

FRET experiments of GSTGFPSp1zfs

It is of advantage in a FRET experiment that the emission spectrum of each GSTGFPSp1zfs overlaps the absorption

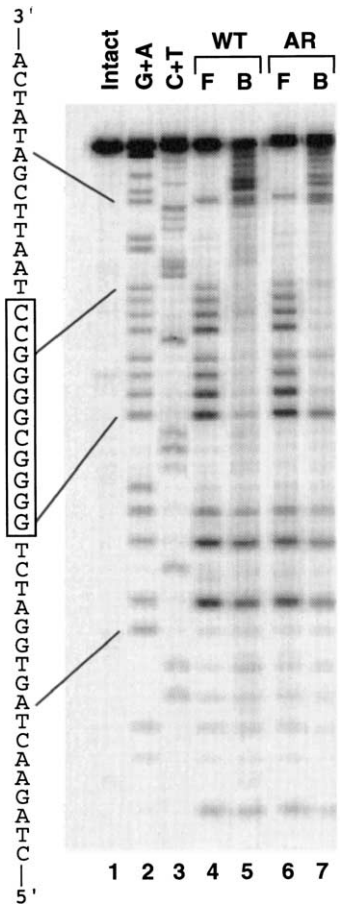

Figure S1. Methylation interference analyses of binding of GSTGFPSp1WT and GSTGFPSp1A556R to the G-strands of the GC-box DNA. Lanes 4 and 6, and lanes 5 and 7 represent peptide-free (F) and peptide-bound (B) DNA samples. Lanes 1–3 contain intact DNA, G and A, and C and T of the Maxam–Golbert reaction,

spectrum of tetrachlorocarboxyfluorescein (TET)-labeled GC-DNA (Fig. 1). Figure 2 exhibits the fluorescence emission spectral changes due to DNA binding of GSTGFPSp1WT or GSTGFPSp1A556R. Arrows in the figure show that the quenching of the emission spectra from GSTGFPSp1zfs is dependent on the concentration of TET-labeled dsDNA. FRET efficiencies

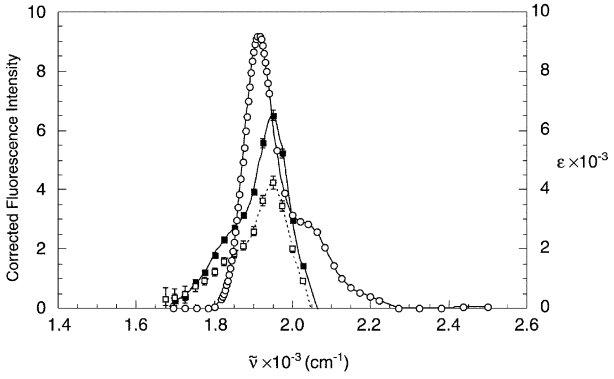

Figure 1. The overlap of corrected fluorescence emission spectra of the donors [GSTGFPSp1WT (closed square) and GSTGFPSp1A556R (open square) in the absence of TET-labeled GC-box DNA] and the absorption spectrum of the acceptor [TET-labeled GC-box DNA (open circle)].

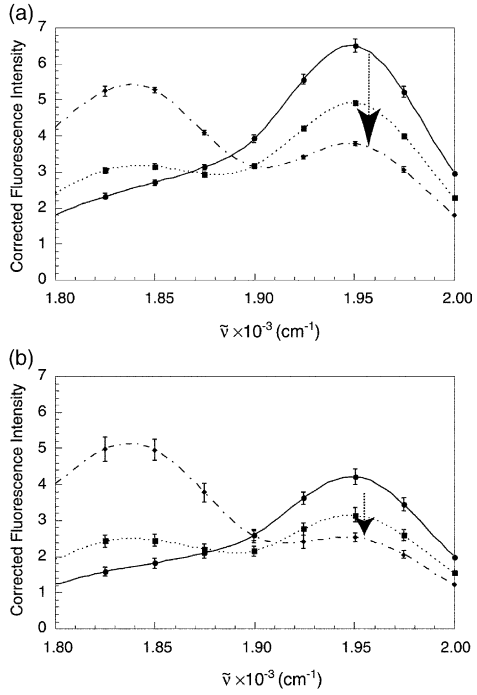

Figure 2. Changes in fluorescence emission spectra of GSTGFPSp1WT (A) or GSTGFPSp1A556R (B) caused by binding to TET-labeled GC-box DNA. The concentrations of added TET-DNA were 0 (circle), 2.5 (square), and 10 (diamond) nM. All plots represent the means of at least three determinations ±SEM.

were determined by the number of quanta transferred from donor to acceptor divided by the number of quanta absorbed by the donor (eq 1). In Figure 3, the saturated E value for TET-labeled dsDNA was treated as that of a one-to-one complex. Table 1 summarizes the various parameters determining the average distance between the GFP and TET fluorophores. The difference between the two distances derived from these two proteins was 1.8 Å when the relative donor–acceptor orientation was randomized rapidly. By considering the difference, the Sp1 finger 1 and the following N-terminal domain might be shifted half-pitch to the 3′-terminus of the G-rich strand by Ala-556→Arg mutation, because of

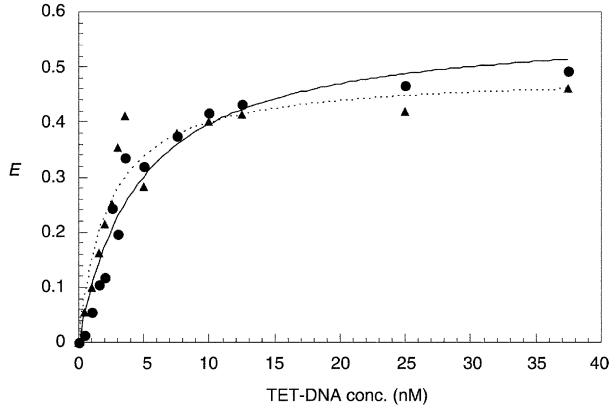

Figure 3. FRET efficiency of GSTGFPSp1WT (circle) or GSTGFPSp1A556R (triangle) versus the concentration of TET-labeled GC-box DNA. The non-linear curve fits are drawn for a 1:1 binding model: E_{max} values of GSTGFPSp1WT and GSTGFPSp1A556R were 0.576 and 0.488, respectively.

Table 1. FRET study parameters for GSTGFPSp1zfs (donor)–TET-labeled GC-box DNA (acceptor) complex[c]

	GSTGFPSp1WT	GSTGFPSp1A556R
Q_{488nm}[a]	0.426	0.375
J ($\times10^{15}$ cm^{-1} M^{-1})[b]	3.44	3.25
R_0[d] (Å)	53.1	51.7
E_{max}[e]	0.576±0.0427	0.488±0.0358
R[f] (Å)	50.6±1.43	52.4±1.24

[a]Calculated at 488 nm by the relative determination using 200 nM Fluorescein in 0.1 N NaOH (Q_{493nm} = 0.92) as the standard sample.
[b]Calculated from eq 3 with the corrected fluorescence intensity, I_D^c.
[c]The fluorescence intensities in the FRET experiments were corrected by the correction factor derived from 100 μM quinine sulfate dissolved in 50 mM sulfuric acid (λ_{365nm}).
[d]Calculated from eq 2.
[e]Obtained by fitting the experimental data to a 1:1 binding model (eq 1 and Fig. 3).
[f]The average distance between the GFP and TET fluorophores (eq 1).

the hydrogen bond formation of Arg with guanine.[11] Unless the rapid randomization of the relative donor–acceptor orientation is assumed, the slight distinction of the orientation in the N-terminal domain is perhaps important as well as the distance. However, the amplitudes of GSTGFPSp1zfs and the error limits of the distance values possibly exclude the different relative orientation or the inter-fluorophore distance of the two mutants.

Steady-state fluorescence anisotropy measurements of GSTGFPSp1zfs

Figure 4 illustrates the plots of the reciprocal number of the anisotropy versus the multiplication of temperature by the fluorescence lifetime. Both r_0 and V values are evaluated from the intercept and slope of the plots (eq 7). Table 2 presents the Perrin equation parameters of GSTGFPSp1zfs in the absence or presence of the GC-box DNA. The volume (114 nm^3) of the GSTGFPSp1A556R–DNA complex was close to that (122 nm^3) of the GSTGFPSp1WT–DNA complex. This result is consistent

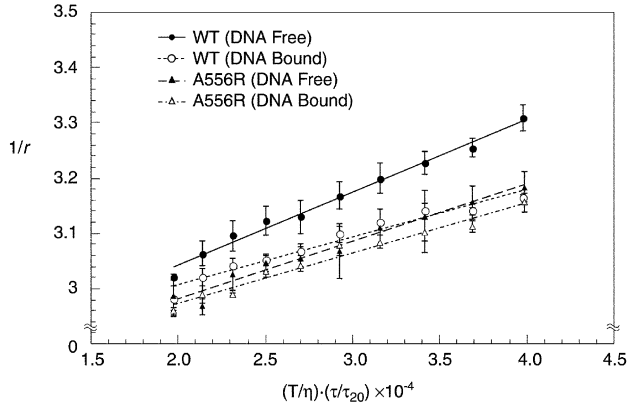

Figure 4. Perrin plots of the dependence of the anisotropy versus the temperature/viscosity for GSTGFPSp1WT (circle) and GSTGFPSp1A556R (triangle) in the presence (open) and absence (closed) of GC-box DNA. On the horizontal axis, the number of the temperature/viscosity was correlated by the ratio of the fluorescence lifetime.

Table 2. The Perrin equation parameters of GSTGFPSp1zfs in the absence or presence of GC-box DNA

Protein	GC box	τ_{20}[a] (ns)	r_0	α[b] (10^{-6}K/P)	V[c] (nm^3)	ΔV[d] (nm^3)
GSTGFPSp1 WT	–	2.69	0.360	13.2	78.2	—
	+	2.69	0.353	8.65	122	43.6
GSTGFPSp1 A556R	–	2.70	0.361	10.4	99.5	—
	+	2.70	0.358	9.10	114	14.8

[a]The fluorescence lifetime was obtained by linear titration for the plots measured at 278, 288, 293, 298, 308 K. Each of the 1–2 μM GSTGFPSp1zfs samples was measured in the buffer containing 10 mM Tris–HCl and 50 mM NaCl, pH 8.0. One component of the fluorescence lifetime was needed only to give an optimal fit. Adding 1 μM GC-box DNA had no effect on the lifetime because of no energy transfer.
[b]The slope ($\alpha = k_B T/r_0 V$) was obtained from a plot of 1/r versus (T/η)·(τ/τ_{20}) (eq 7 and Fig. 4). The viscosity of water was used as η (e.g., η (20 °C) = 1.002 cP).
[c]The hydrodynamic volume of the rotating unit based on the assumption that the molecules are spherical. 1 P is 0.1 N s m^{-2} and the Boltzmann constant (k_B) is 1.38×10^{-23} N s K^{-1}·m^{-2} (eq 7).
[d]The alterations of V was involved in the complex formation of GSTGFPSp1zfs for GC-box DNA.

with the correspondence between two donor–acceptor distances shown by FRET, suggesting that the different DNA binding modes of the zinc finger domain of these proteins have no significant effect on the geometry of the adjacent N-terminal domain in DNA binding. The difference in the two DNA-free forms was significant, and GSTGFPSp1WT ($V = 78.2$ nm^3) was more compact than GSTGFPSp1A556R (99.5 nm^3). Consequently, the altered amount ($\Delta V = 43.6$ nm^3) of the volume of GSTGFPSp1WT by DNA binding was much larger than that (14.8 nm^3) of GSTGFPSp1A556R. This volume corresponds with approximately twice the inherent volume of 15 bp dsDNA (about 5.5 nm^3; anticipation by WebLab^{TM} ViewerLite). Probably, GSTGFPSp1WT is folded compactly through the native finger 1 region, and DNA binding induces a favorable N-terminal conformation with a drastic change. In contrast, GSTGFPSp1A556R has an extended form, and DNA binding does not alter the N-terminal conformation.

Implications for N-terminal zinc finger of Sp1 and Sp/XKLF family members as hinge finger

In eukaryotic transcription, the existence of large families of sequence-specific activators as well as a host of accessory factors is necessary to form a functional RNA polymerase II complex.[30] All Sp/KLF family members conserve three homologous zinc fingers on the C-terminus and also an alanine residue at position 6 on the N-terminal finger recognition helix. However, the members have various lengths and kinds of domains at the N-terminus linking to the zinc finger.[31–33] In the N-terminus of Sp1, the domains A and B containing Glu- and Ser/Thr-rich segments associate with $TAF_{II}110$[34,35] and also cause a tetrameric assembly that induces DNA looping.[36–38] It is of interest what roles the conserved C-terminal three zinc fingers, particularly N-terminal zinc finger, of Sp/XKLF family members play.

Cooperative interactions of regulators with their targets are necessary to the on–off switch for the transcription of specific genes. In the Sp/KLF family, the binding sequence diversity of the N-terminal zinc finger 1 is applicable to expressing various genes with diverse GC-rich sequences. Accordingly, it seems that the allosteric control is not regulated significantly by the DNA sequence. Some Sp1 sites appear singly and others continuously in various gene promoters, and their locations are not conserved. Sp1 sites in a promoter can respond to multiple Sp/KLF family members or a particular one in a cell type, and in different promoters, can respond differently in the same cell. Specific transcriptional activities of the members depend dominantly on the shapes and functions of the N-terminal regulation domains that specifically interact with various ambient factors.[39] A cooperative process requires a conformational change by binding one substrate and a subsequent change in affinity for the other substrates. This study shows that DNA binding of Sp1 containing the unique N-terminal finger 1 is attended by a conformational change in the adjacent N-terminal domain. In the Sp/XKLF family, DNA binding might regulate the binding of the N-terminal regulation domain to the other transcriptional factors and also perform transcription of each specific gene. A flexible hinge between functional domains (e.g., enzymatic activity, DNA binding, ligand binding and cluster formation) is essential for various mechanisms.[40–46] Presumably, the 'hinge finger' is necessary to facilitate the interaction with GC-rich DNA and various regulators. The comparison of transcriptional activity between two full-length proteins, the Sp1 wild type and the Ala-556→Arg mutant, or the investigation of the fluctuation of the adjacent N-terminal domain will clarify the hinge activity of the N-terminal zinc finger 1.

Experimental

Preparation of GSTGFPSp1zfs

The construction of the coding vector of GSTGFPSp1zfs was as follows. The coding region of EGFP, the enhanced GFP protein (F64L, S65T),[24] was amplified by PCR for pEGFP-N1 (CLONTECH) using the sequences 5′-CGC CAC CAT GGT GAG CAA GGG C-3′ for the forward and 5′-GTC GGA ATT CTA AGG ATC CTT GTA CAG CT-3′ for the reverse. The PCR fragment was inserted into the *Nco*I/*Eco*RI site of pET42b to construct pEVGSTGFP which codes the glutathione-*S*-transferase-tag (GST-tag) linking to the N-terminus of EGFP. The pEVSp1zfs, namely pEVSp1(530–623) and pEVSp1A556R,[11] were double-digested with *Bam*HI and *Eco*RI. The fragments were cloned in frame into the same sites of pEVGSTGFP, generating the GST-EGFP fusion protein linking to the N-terminus of the Sp1 zinc-finger region. The expression of GSTGFPSp1zfs was proceeded as previously described.[7,9,11] The sonicated cells in PBS buffer were centrifuged, and then the supernatants containing GSTGFPSp1zfs were loaded onto the GSTrap column (Amersham Biosciences) and eluted with the elution buffer containing 50 mM Tris–HCl and 10 mM reduced glutathione, pH 8.0. The purified proteins were dialyzed

with Tris–NaCl containing glycerol (TNG) buffer and diluted moderately. DC Protein Assay (Bio-Rad) determined the concentrations of these proteins.

Gel mobility-shift assay

The probe DNAs (41 bp *Hind*III-*Xba*I fragments) were prepared as previously described.[7,11] The bands were visualized by autoradiography and quantitated with the ImageMaster (Amersham Biosciences).

Methylation interference experiments

Methylation interference analyses were performed according to previous papers for the determination of the DNA binding mode.[7]

Preparation of TET-labeled DNA

All oligonucleotides were purchased from Amersham Biosciences. The C-rich strand oligonucleotide, 5′-AAT TAG GCC CCG CCC CAG A-3′, was labeled with TET on the 5′-terminus, and the G-rich strand one, 5′-TCT GGG GCG GGG CCT AAT T-3′, was not labeled. These oligonucleotides were used after annealing. For steady-state anisotropy and fluorescence lifetime measurements, 5′-TAG GCC CCG CCC CAG-3′ and 5′-TCT GGG GCG GGG CCA-3′ were each annealed.

FRET

Steady-state fluorescence spectroscopy was performed at 20 °C on a Hitachi F-3010 spectrofluorometer with excitation at 488 nm using an excitation and emission band-pass of 1.5 and 3.0 nm, respectively. The absorbance of the samples was below 0.05 at the excitation wavelength, so the inner filter effect was negligible. Quantum yields were measured using 200 nM fluorescein in 0.1 N sodium hydrate, and the corrected fluorescence intensities were determined by the corrected function based on 10 μM quinine sulfate in 50 mM sulfuric acid. Each 100 nM GSTGFPSp1zfs sample was incubated at 20 °C for an hour with TET-labeled double-stranded oligonucleotide in the binding buffer containing 10 mM Tris–HCl (pH 8.0) and 50 mM NaCl. The FRET efficiency (E) was calculated from the acceptor-induced change in the fluorescence intensity of the donor as:

$$E = 1 - \frac{I_{DA}}{I_D} = \frac{R_O^6}{R^6 + R_O^6} \quad (1)$$

where I_{DA} and I_D are the fluorescence intensities of the donor molecules in the presence and absence of the acceptor, respectively.[15,16] Förster's critical distance (R_O, expressed in Å) is defined as the donor–acceptor distance where the FRET efficiency is 50%. The donor–acceptor distance (R) is isolated from E and R_O. The value of R_O is obtained using the following equation:

$$R_O^6 = (8.79 \times 10^{-11}) n^{-4} \kappa^2 Q_D J \quad (2)$$

where n is the refractive index of the medium, κ^2 is the orientation factor of the transition dipole moments, Q_D is the fluorescence quantum yield of the GSTGFPSp1zfs in the absence of an acceptor, and J is the overlap integral. The refractive index (n) was assumed to be 1.4 for the aqueous solution. The orientation factor (κ^2) was assumed to be equal to 2/3 for rapid randomization of the relative donor–acceptor orientation. The overlap integral (J) is defined as:

$$J = \int_{\infty}^{0} I_D(\lambda)\varepsilon_A(\lambda)\lambda^4 d\lambda \quad (3)$$

where $I_D(\lambda)$ is the corrected fluorescence emission intensity of the donor and $\varepsilon_A(\lambda)$ is the extinction coefficient of the acceptor.[15,16]

Steady-state anisotropy measurements

The fluorescence spectroscopy for anisotropy was performed on a Hitachi F-4500 spectrofluorometer equipped with a polarization accessory. The excitation and emission wavelengths were 480 and 515 nm, respectively, using a band-pass of 10 nm. Fluorescence anisotropy (r) was calculated from fluorescence intensity measurements by vertical polarized excitation beams with vertically (I_{VV}) and horizontally (I_{VH}) polarized emission light according to

$$r = \frac{I_{VV} - G \cdot I_{VH}}{I_{VV} + 2G \cdot I_{VH}} \quad (4)$$

where the factor $G = I_{HV}/I_{HH}$ corrects the measured intensities for differences in the sensitivity of the detection of vertically and horizontally polarized excitation light.[18] Each sample (3 mL) contained 10 mM Tris–HCl (pH 8.0), 50 mM NaCl, and 50 nM GSTGFPzfs, in the presence or absence of 500 nM non-labeled double-stranded DNA (dsDNA). Each anisotropy was measured at least three times at each temperature, in steps of 3 °C from 5 to 35 °C. The anisotropy was fitted to the Perrin equation for each sample,[17,18]

$$\frac{1}{r} = \frac{1}{r_o}\left[1 + \frac{\tau}{\theta}\right] \quad (5)$$

where r_o is the initial anisotropy and θ is the fluorescence rotational correlation time described by the Stokes–Einstein equation,

$$\theta = \frac{\eta V}{k_B T} \quad (6)$$

where k_B, τ, V, and η are the Boltzmann constant, the excited-state lifetime, the hydrodynamic volume of the rotating molecule, and the viscosity of water, respectively. When eq 6 is substituted into eq 5, the following equation is obtained.

$$\frac{1}{r} = \frac{1}{r_0}\left[1 + \frac{k_B T \tau}{\eta} \cdot \frac{1}{V}\right] \quad (7)$$

Fluorescence lifetime measurements

Fluorescence lifetimes were measured by a time-correlated single-photon counting method on a Horiba multi-channel-TAC NAES-550 system. The probe was excited through an interference filter (Optical Coatings Japan, MIF-W, 480.9 nm, $\lambda_{1/2} = 11.9$ nm) and detected through a cutoff filter (Hoya, Y51) and a liquid filter ($NiSO_4 \cdot 6H_2O$, 500 g/L). The instrument response time was 1 ns [full width half maximum (FWHM)]. The total fluorescence decay $S(t)$ was analyzed using an exponential decay function with the fraction amplitudes α_i and the lifetimes τ_I.[47]

$$S(t) = \sum_{i=1}^{n} \alpha_i \exp\left(-\frac{t_i}{\tau_i}\right) \quad (8)$$

10,000 Photons were collected in the peak channel. The fitting of a single component decay of the fluorescence lifetime was needed only to provide an optimal fit. The quality of the fit was judged by the χ^2 value, the reduced chi square parameter.

Acknowledgements

Gratitude is due to Professor Tetsuro Handa and Mr. Atsuhiko Sugita, Kyoto University, for helpful suggestions in determination of the fluorescence anisotropy and lifetimes. We also thank Dr. Makoto Nagaoka, Kyoto University, for helpful discussion. This study was supported in part by a Grant-in-aid for the COE Project 'Element Science', Priority Project 'Biometals', and Scientific Research from the Ministry of Education, Culture, Sports, Science, and Technology, Japan.

References and Notes

1. Dynan, W. S.; Tjian, R. *Cell* **1983**, *32*, 669.
2. Kadonaga, J. T.; Jones, K. A.; Tjian, R. *Trends Biochem. Sci.* **1986**, *11*, 20.
3. Bucher, P. *J. Mol. Biol.* **1990**, *212*, 563.
4. Berg, J. M. *Proc. Natl. Acad. Sci. U.S.A.* **1992**, *89*, 11109.
5. Kriwacki, R. W.; Schultz, S. C.; Steitz, T. A.; Caradonna, J. P. *Proc. Natl. Acad. Sci. U.S.A.* **1992**, *89*, 9759.
6. Kuwahara, J.; Yonezawa, A.; Futamura, M.; Sugiura, Y. *Biochemistry* **1993**, *32*, 5994.
7. Yokono, M.; Saegusa, N.; Matsushita, K.; Sugiura, Y. *Biochemistry* **1998**, *37*, 6824.
8. Shi, Y.; Berg, J. M. *Chem. Biol.* **1995**, *2*, 83.
9. Uno, Y.; Matsushita, K.; Nagaoka, M.; Sugiura, Y. *Biochemistry* **2001**, *40*, 1787.
10. Choo, Y. *Nucleic Acids Res.* **1998**, *26*, 554.
11. Matsushita, K.; Sugiura, Y. *Bioorg. Med. Chem.* **2001**, *9*, 2259.
12. Hillisch, A.; Lorenz, M.; Diekmann, S. *Curr. Opin. Struct. Biol.* **2001**, *11*, 201.
13. Jamieson, E. R.; Jacobson, M. P.; Barners, C. M.; Chow, C. S.; Lippard, S. J. *J. Biol. Chem.* **1999**, *274*, 12346.
14. Schmid, J. A.; Birbach, A.; Hofer-Warbinek, R.; Pengg, M.; Burner, U.; Furtmüller, P. G.; Binder, B. R.; de Martin, R. J. *Biol. Chem.* **2000**, *275*, 17035.
15. Stryer, L. *Ann. Rev. Biochem.* **1978**, *47*, 819.
16. Clegg, R. M. In *Fluorescence Imaging Spectroscopy and Microscopy*; Wang, X. F., Herman, B., Eds.; Wiley: New York, 1996; p 179.
17. Weber, G. *Adv. Protein Chem.* **1953**, *8*, 415.
18. Lakowicz, J. R. In *Principle of Fluorescence Spectroscopy*, 2nd ed.; Plenum: New York, 1999; p 291.
19. Hantgan, R. R. *Biochemistry* **1982**, *21*, 1821.
20. LeTilly, V.; Royer, C. A. *Biochemistry* **1993**, *32*, 7753.
21. Albani, J. R. *Biochim. Biophys. Acta* **1997**, *1336*, 349.
22. Shimomura, O.; Johnson, F. H.; Saiga, Y. *J. Cell. Comp. Physiol.* **1962**, *59*, 223.
23. Morise, H.; Shimomura, O.; Johnson, F. H.; Winant, J. *Biochemistry* **1973**, *13*, 2656.
24. Tsien, R. Y. *Annu. Rev. Biochem.* **1998**, *67*, 509.
25. Chalfie, M.; Tu, Y.; Euskirchen, G.; Ward, W. W.; Prasher, D. C. *Science* **1994**, *263*, 802.
26. White, J.; Stelzer, E. *Trends Cell Biol.* **1999**, *9*, 61.
27. Pollok, B.; Heim, R. *Trends Cell Biol.* **1999**, *9*, 57.
28. Heim, R. *Method Enzymol.* **1999**, *302*, 408.
29. Nagai, Y.; Miyazaki, M.; Aoki, R.; Zama, T.; Inouye, S.; Hirose, K.; Iino, M.; Hagiwara, M. *Nat. Biotechnol.* **2000**, *18*, 313.
30. Lemon, B.; Tjian, R. *Genes Dev.* **2000**, *14*, 2551.
31. Philipsen, S.; Suske, G. *Nucleic Acids Res.* **1999**, *27*, 2991.
32. Dang, D. T.; Pevsner, J.; Yang, V. W. *Int. J. Biochem. Cell Biol.* **2000**, *32*, 1103.
33. Turner, J.; Crossley, M. *Trends Biol. Sci.* **1999**, *9*, 57.
34. Hoey, T.; Gill, G.; Chen, J. L.; Dynlacht, B. D.; Tjian, R. *Cell* **1993**, *72*, 247.
35. Gill, G.; Pascal, E.; Tseng, Z. H.; Tjian, R. *Proc. Natl. Acad. Sci. U.S.A.* **1994**, *91*, 192.
36. Courey, A. J.; Tjian, R. *Cell* **1988**, *55*, 887.
37. Mastrangelo, I. A.; Courey, A. J.; Wall, J. S.; Jackson, S. P.; Hough, P. V. C. *Proc. Natl. Acad. Sci. U.S.A.* **1991**, *88*, 5670.
38. Su, W.; Jackson, S.; Tjian, R.; Echols, H. *Genes Dev.* **1991**, *5*, 820.
39. Black, A. R.; Black, J. D.; Azizkhan-Cliffford, J. *J. Cell. Physiol.* **2001**, *188*, 143.
40. Ghost, G.; van Duyne, G.; Ghost, S.; Sigler, P. B. *Nature (London)* **1995**, *373*, 303.
41. Nagadoi, A.; Nakazawa, K.; Uda, H.; Okuno, K.; Maekawa, T.; Ishii, S.; Nishimura, Y. *J. Mol. Biol.* **1999**, *287*, 593.
42. Lewis, M.; Chang, G.; Horton, N. C.; Kercher, M. A.; Pace, H. C.; Schumacher, M. A.; Brennan, R. G.; Lu, P. *Science* **1996**, *271*, 1247.
43. Spronk, C. A. E. M.; Folker, G. E.; Noordman, A.-M. G. W.; Wechselberger, R.; van den Brink, N.; Boelens, R.; Kaptein, R. *EMBO J.* **1999**, *18*, 6472.
44. Antson, A. A.; Burns, J. E.; Moroz, O. V.; Scott, D. J.; Sanders, C. M.; Bronstein, I. B.; Dodson, G. G.; Wilson, K. S.; Maitland, N. J. *Nature (London)* **2000**, *403*, 805.
45. Zou, N.; Lin, B. Y.; Duan, F.; Lee, K. Y.; Jin, G.; Guan, R.; Yao, G.; Lefkowitz, E. J.; Broker, T. R.; Chow, L. T. *J. Virol.* **2000**, *74*, 3761.
46. Wang, Q.; Lu, J. H.; Yong, E. L. *J. Biol. Chem.* **2001**, *276*, 7493.
47. Saito, H.; Minamida, T.; Arimoto, I.; Handa, T.; Miyajima, K. *J. Biol. Chem.* **1996**, *271*, 15515.